Experimental report

06/09/2019

Proposal:	**4-01-1597**	**Council:**	10/2018

Title: Longitudinal polarization analysisof the non-reciprocal magnons in the skyrmion, conical and field-polarized phases of MnSi

Research area: Physics

This proposal is a new proposal

Main proposer: **Tobias WEBER**

Experimental team: Tobias WEBER

Local contacts: Paul STEFFENS

Samples: MnSi

Instrument	Requested days	Allocated days	From	To
THALES	9	6	28/06/2019	04/07/2019

Abstract:

We recently completed our study into magnon dynamics in all magnetically ordered phases of the itinerant magnet MnSi, including the conical, the field-polarized and the skyrmion phase. The main result was the identification of non-reciprocal (asymmetric) dynamics in all of the individual phases. Even with all of our previous scans being unpolarized, our theoretical model predicts a re-shuffling of spectral weights between the polarization channels as a mechanism of the observed asymmetries. With longitudinal polarization analysis and the high flux at Thales we wish to resolve these theoretical observations.

Recently, we performed a two-day internal test experiment and feasibility study for longitudinal polarization analysis of the skyrmion dynamics at Thales (see attached report INTER-413), which yielded highly promising results, clearly showing a separation of the non-reciprocal magnons in the skyrmion phase into the two spin-flip channels.

Due to the importance of the experiments and the strong competition, we ask to continue our initial internal studies optimally using nine days of beamtime (minimally six days would be sufficient).

Longitudinal polarization analysis in MnSi

T. Weber,[1,*] P. Steffens,[1] M. Böhm,[1] A. Bauer,[2] J. Waizner,[3] C. Pfleiderer,[2] P. Böni,[2] and M. Garst[4]

[1] *Institut Laue-Langevin (ILL), 71 avenue des Martyrs, 38000 Grenoble, France*
[2] *Physik-Department E21, Technische Universität München (TUM), James-Franck-Str. 1, 85748 Garching, Germany*
[3] *Institut für Theoretische Physik, Universität zu Köln, Zülpicher Str. 77a, 50937 Köln, Germany*
[4] *Institut für Theoretische Festkörperphysik, Karlsruhe Institute of Technology, 76131 Karlsruhe, Germany*
(Dated: September 6, 2019)

The itinerant-electron compound MnSi features several magnetically ordered and disordered phases. Among the ordered are the helical [1, 2], conical [3], field-polarized ferromagnetic [4] and skyrmion phase [5, 6]. The disordered phases include the fluctuation-disordered [7] and the paramagnetic [8] phase. At the boundary between the conical, the field-polarized and the fluctuation-disordered phases a tri-critical point [9] is found.

In the following we phenomenologically describe the current version of our theoretical model [10], which is being developed alongside our experiments. The non-centrosymmetric P$2_1$3 space group of MnSi has profound consequences for spin-wave dynamics in all these phases. Namely, it introduces a Dzyaloshinskii-Moriya term which – at reduced momentum transfers parallel to the external magnetic field direction – causes magnons to be created at different (absolute) energies than they are annihilated and furthermore leads to different spectral weights for magnon creation compared to annihilation. The resulting dynamical magnetic structure factors $S(\boldsymbol{q}, E)$ with $\boldsymbol{q} = \boldsymbol{Q} - \boldsymbol{G}$ are thus asymmetric ("non-reciprocal") as long as the reduced momentum transfer $\boldsymbol{q}$ from the neutron to the magnon has a component $\boldsymbol{q}_{\parallel}$ along the direction of the external magnetic field $\boldsymbol{B}$. The dispersion for $\boldsymbol{q}_{\parallel} \parallel \boldsymbol{B}$ is depicted for the skyrmion, conical, and field-polarized phase as panels (a) in Figs. 1, 2, and 3, respectively. In the conical phase, Fig. 2 (a), the dispersion comprises two sets of parabola centered around the two helimagnetic satellite reflections. Due to non-reciprocity, these parabola have different spectral weights for magnon creation compared to annihilation [3]. In the skyrmion-phase, the parabola split into a multitude of complicated sub-modes, Fig. 1 (a), whereas is the field-polarized phase, Fig. 3 (a), only one parabola remains for either magnon creation or annihilation, making the dispersion fully asymmetric. Moreover, the dispersion branches are not centered around the nuclear (110) reflection, but have their minimum at the positions in reciprocal space were the magnetic satellites were located in the helical/conical phase. The thin gray lines in Fig. 1 signify modes whose eigenvalues exist, but which have no spectral weight, as determined by the corresponding eigenvector.

In stark contrast to the non-reciprocal spectra, the dispersions are symmetric for reduced momentum transfers

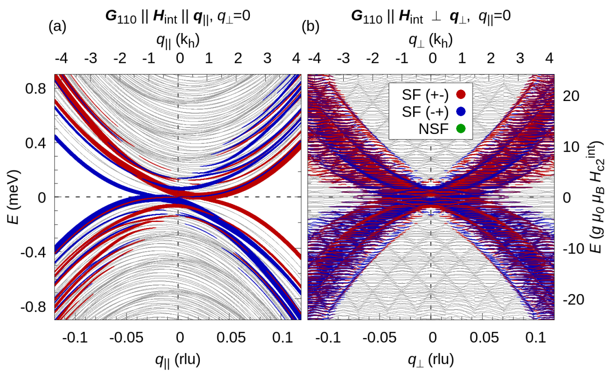

Figure 1. Theoretical [10] polarization-dependent magnon dispersion in the skyrmion phase.

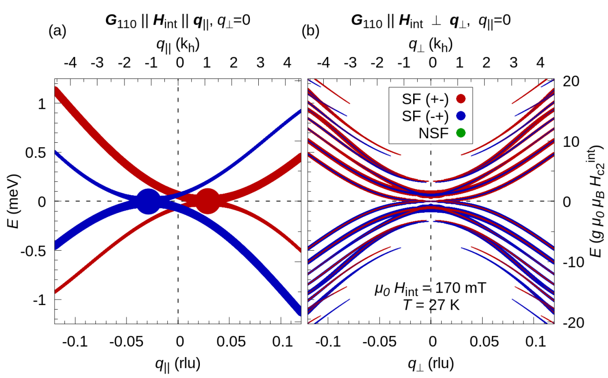

Figure 2. Theoretical [10] polarization-dependent magnon dispersion in the conical phase [3].

perpendicular to the applied magnetic field, $\boldsymbol{q}_{\perp}$, as depicted in the panels (b) of Figs. 1, 2, and 3. In the conical case, Fig. 2 (b), they lead to the formation of a band structure [1, 2] due to a back-folding of the spectra into the first magnetic Brillouin zone. In the field-polarized phase, Fig. 3 (b), these bands converge towards one parabolic, ferromagnetic mode. The most interesting case is the behavior in the skyrmion phase, Fig. 1 (b). Here, the discrete bands of the conical phase smear out towards a broad continuum of states.

We investigated the separation into spin-flip and non-spin-flip channels of the non-reciprocal magnons in the skyrmion, conical, and field-polarized phase of MnSi using the instrument Thales [11]. At Thales, neutrons leave the Heusler monochromator in a spin-down state and are

* Correspondence: tweber@ill.fr

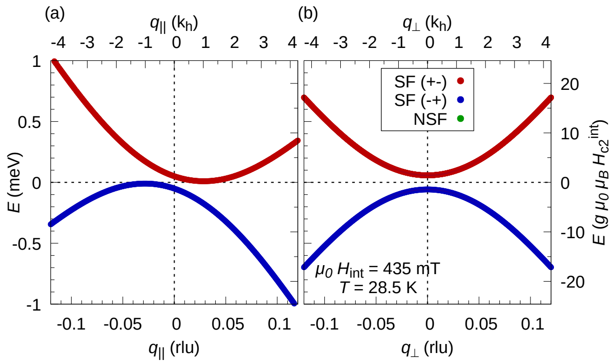

Figure 3. Theoretical [10] polarization-dependent magnon dispersion in the field-polarized phase.

guided by a field with its north-pole pointing upwards towards the sample. Close to the sample, the guide field changes adiabatically into the horizontal plane with normal direction [001]. At the Heusler analyzer, only the spin-down state passes. In our notation "SF (+-)" means that the neutron spin is flipped at the k_i axis towards the spin-up state, is again flipped at the sample towards the spin-down state, and is analyzed in that state. For "SF (-+)", the neutron enters the sample in the spin-down state, is flipped at the sample, enters the k_f axis in spin-up, is flipped towards spin-down at the second Mezei flipper and analyzed. "NSF" denotes the state where the neutron remains in the spin-down state.

The measurements were performed in the $(hk0)$ scattering plane around the nuclear $\boldsymbol{G} = (110)$ reflection with the magnetic field oriented along [110]. In this configuration, the skyrmion plane is spanned by the $[1\bar{1}0]$ and [001] reciprocal vectors and the hexagonal skyrmion lattice pins along $[1\bar{1}0]$. In the conical/helical phase, the incommensurate magnetic structure is observed by two magnetic satellites of opposing polarization which are oriented along the field direction at distances given by the helix pitch $k_h = 2\pi/\lambda_h$. None of the other phases possesses incommensurate magnetic satellite reflections.

Figs. 4, 5, 6, and 7 show the experimental results in skyrmion, conical and fluctuation-disordered as well as at the tri-critical point, respectively. Each column of figures corresponds to the same scan position for each phase, where columns 1 and 2 show the non-reciprocal dynamics for the $\boldsymbol{q}_{||} \parallel \boldsymbol{B}$ direction, and column 3 the symmetric dynamics for $\boldsymbol{q}_\perp \perp \boldsymbol{B}$. The lines in all figures merely serve as guides to the eye. Each phase show the same basic structure of the dispersion: Non-reciprocal peaks which flip in energy upon reversal of $\boldsymbol{q}_{||}$ (columns 1 and 2) and broad spectra for reduced momenta perpendicular to the applied field direction (column 3).

We succeeded in mapping out the non-reciprocal dynamics in the various magnetic phases of MnSi and started investigating the broad features in the symmetric $\boldsymbol{q}_\perp$ dispersions. The convolution-based data analysis for the conical phase was recently finished and led to a beautiful match between theory and experiment. Our results for the conical phase were published a few weeks ago as a PRB Rapid Communication [3]. The convolutions for the skyrmion and field-polarized phases led to equally perfect matches, for which two upcoming papers, one for the dynamics in each phase, are currently in preparation.

Within the resolution of the setup that we employed – a horizontally and vertically focusing monochromator, a vertically focusing analyzer and one 30 minutes collimator in the k_f axis – the finer details of the individual dispersion relations are unfortunately not immediately discernible without a resolution-convolution of the theoretical models (not shown). For future investigations we will follow two threads: (1) While our model works very well for the conical, skyrmion, and field-polarized phase, we do not yet have a working spin-wave theory for the fluctuation-disordered and paramagnetic phase or for the tri-critical point. We will thus require a continuation beamtime to further investigate the exact differences between the dispersions in the individual phases in more detail. (2) As the dispersions in the skyrmion and field-polarized phases are not centered on the nuclear Bragg peak, they are well-accessible for low-energy measurements. It would therefore be worthwhile to use these low-E modes for a ferromagnetic spin-echo experiment to determine the magnon lifetimes and help extend our model towards predicting linewidths. At the moment, it does not yet consider any Gilbert damping.

We are very grateful for the technical support by E. Villard and P. Chevalier. We furthermore owe many thanks to G. Brandl and M. Kugler for their original Python implementations of the helimagnon [2, 10] and early version of the skyrmion model [10] upon which our code has initially been based. Data DOI: 10.5291/ILL-DATA.4-01-1597.

[1] M. Janoschek *et al.*, Phys. Rev. B **81**, 214436 (2010).
[2] M. Kugler *et al.*, Phys. Rev. Lett. **115**, 097203 (2015).
[3] T. Weber *et al.*, Phys. Rev. B **100**, 060404 (2019).
[4] T. J. Sato *et al.*, Phys. Rev. B **94**, 144420 (2016).
[5] S. Mühlbauer *et al.*, Science **323**, 915 (2009).
[6] M. Janoschek *et al.*, Journal of Physics: Conference Series **200**, 032026 (2010).
[7] M. Janoschek *et al.*, Phys. Rev. B **87**, 134407 (2013).
[8] B. Roessli *et al.*, Phys. Rev. Lett. **88**, 237204 (2002).
[9] A. Bauer *et al.*, Phys. Rev. Lett. **110**, 177207 (2013).
[10] M. Garst *et al.*, Journal of Physics D: Applied Physics **50**, 293002 (2017).
[11] M. Böhm *et al.*, Neutron News **26**, 18 (2015).

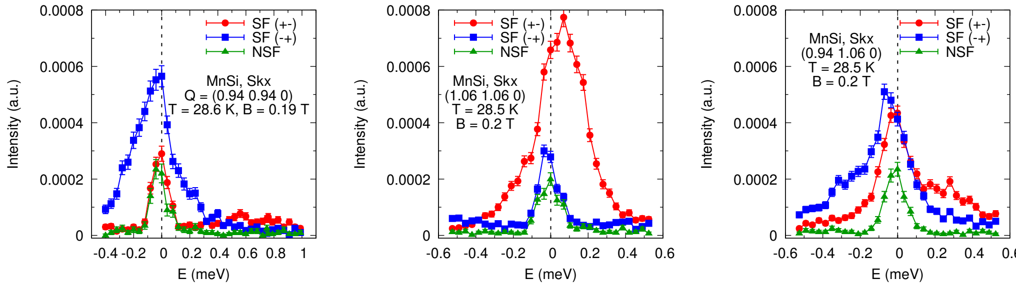

Figure 4. Polarized energy scan at $\boldsymbol{Q}_{\|,1} = (0.94\ 0.94\ 0)$, $\boldsymbol{Q}_{\|,2} = (1.06\ 1.06\ 0)$ and $\boldsymbol{Q}_{\perp} = (0.94\ 1.06\ 0)$ in the skyrmion phase. The first two scans show the non-reciprocal dynamics. The third one the ensuing continuum of states. The following figures show the same scans in the other magnetic phases.

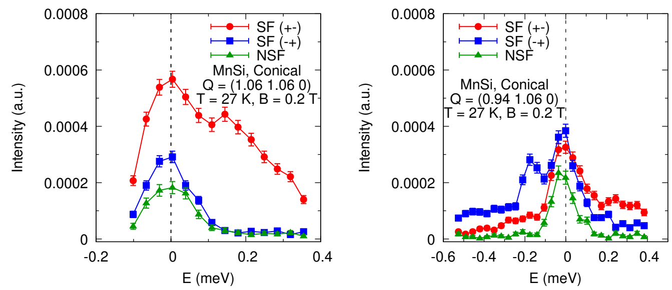

Figure 5. Polarized energy scan at $\boldsymbol{Q}_{\|,2} = (1.06\ 1.06\ 0)$ and $\boldsymbol{Q}_{\perp} = (0.94\ 1.06\ 0)$ in the conical phase [1, 2]. The first scan depicts the non-reciprocal dynamics. The second one shows the onset of the discrete helimagnon bands. We very recently published these results [3].

Figure 6. Polarized energy scan at $\boldsymbol{Q}_{\|,1} = (0.94\ 0.94\ 0)$ and $\boldsymbol{Q}_{\perp} = (1.06\ 0.94\ 0)$ in the fluctuation-disordered phase [7]. The first scan exhibits a similar non-reciprocity as observed in the conical and skyrmion phase, albeit shifted towards lower absolute energies. Low-energy excitations can be detected in the second scan.

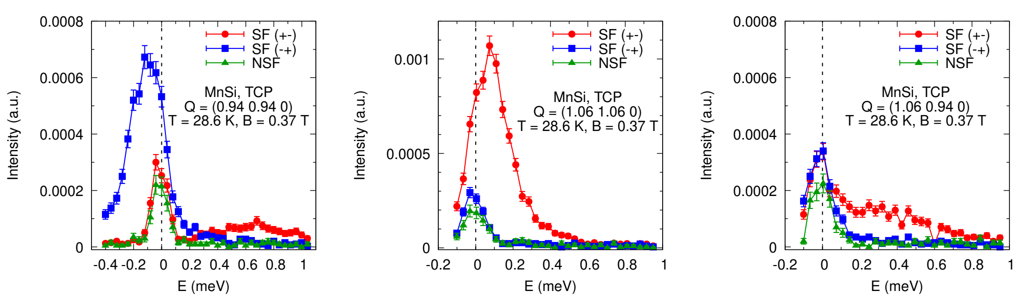

Figure 7. Polarized energy scan at $\boldsymbol{Q}_{\|,1} = (0.94\ 0.94\ 0)$, $\boldsymbol{Q}_{\|,2} = (1.06\ 1.06\ 0)$ and $\boldsymbol{Q}_{\perp} = (1.06\ 0.94\ 0)$ at the tri-critical point [9]. The first two scans exhibit non-reciprocal dynamics similar to the conical and skyrmion phase. The third scan shows a broad spectrum of excitations.